A NEW DESIGN PRINCIPLE FOR DAMAGE TOLERANT STRUCTURAL BONDING IN AEROSPACE APPLICATIONS

Martin Blacha, Airbus Helicopters, Donauwörth, Germany
Thomas Joachim, Airbus Helicopters, Donauwörth, Germany

Abstract

The main obstacle of introducing structural bondings in aerospace applications is its damage tolerance behavior as in case of damages a potential crack can grow in an un-controlled manner to a critical size. At Airbus Helicopters a purely geometrical adaption of a single lap shear bond line was developed which stops a potential crack-growth effectively and reliably. The main principle is based upon splitting up the bond line along its length into several sub-bondings. The separation of the individual sub-bondings is achieved by an intermeshing pattern of both ends of the panels (for example a zig-zag-line) which are connected to the splice plate. At this zig-zag line cracks cannot propagate anymore and thus are stopped effectively. Additional benefit of the intermeshing pattern is that the stress peaks are reduced significantly compared to the common constant overlap. It is demonstrated by analysis and test that the new design principle is limiting crack growth in the bond line and increases the load transfer capability at the same time.

1. NOTATION

Symbols

F	force, N
M	(bending) moment, Nm
σ	tension stress, MPa
τ	shear stress, MPa

Acronyms:

BVID	Barely visible impact damage
CFRP	Carbon Fiber Reinforced Plastics
ERF	European Rotorcraft Forum
FE	Finite Element
FAL	Final Assemble Line
FRP	Fiber Reinforced Plastics
H/W	Hot and wet
LL	Limit load
LuFo	German “Luftfahrt Forschung” national research funding
RTA	Room temperature ambient
SLS	Single lap shear
UL	Ultimate Load

2. INTRODUCTION

Due to its high requirements with respect to safety and reliability structural bonding in aerospace applications faces several challenges in different fields: Starting with a proper selection of suitable adhesives with a wide range of environmental conditions and the complete process adherence including quality control. But even with respecting all these requirements, principles, and processes there is still the threat that in case of imperfections or local damages during operation, cracks in the bond line might occur and propagate undetected to a size which endangers safe operation of the aircraft.

Thus, in order to establish a certifiable structural bonding in general several criteria have to be fulfilled: At first a dedicated traceable and reliable, bonding process needs to be established and followed in order to be reproducible and exclude the human factor. Then a thorough quality program needs to be established in order to ensure the requested strength of the bonding. And finally, under any in-service operational condition an undetected or uncontrolled crack growth has to be excluded in a reliable manner which is up to now the missing key feature in bond-lines for certification.

This publication focusses on the aspect of the development of exactly this key feature in order to establish the damage-tolerance of the bond line itself. Goal is to introduce a very simple and effective means to stop crack growth effectively without compromising the structural strength of the bonding. This is done based upon a simple geometric modification of the shape in the bond line. On top, the principle described here can be in general transferred to any joining method based upon positive substance jointing as for example brazing, co-bonding of FRP structures, thermoplastic welding, film diffusion joining, etc.

All research work presented in this publication was performed in the frame of the German funded LuFo research project "JoinDT" in cooperation with industry and research partners.

3. Basic description of the design principle

3.1. State of the art design principle for single lap shear joining

The principles of design and analysis especially for lap shear connections is well known for decades and is well described and examined, see Ref. 1 and Ref. 2. These descriptions of the general principle for lap-shear joints are in use for many decades now and are shown as general design principle in Figure 1 and Figure 2.

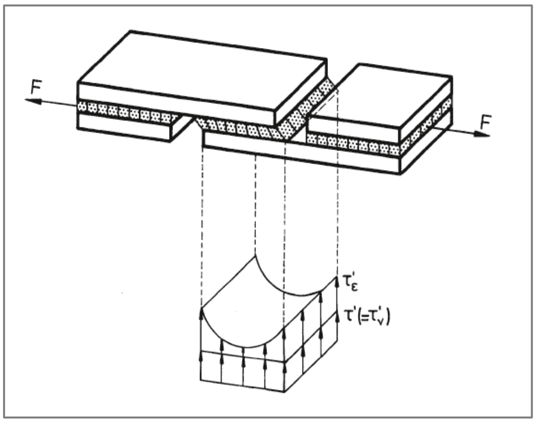

Figure 1: Principle of shear stress distribution in typical lap-shear joints, Ref. 6.

There is a significant difference between the stresses shown in the two figures: in Figure 1 the pure shear stresses resulting from the transfer of the external force F is shown. As due to the offset of the two substrates a moment is generated in the bonded joint, additional peel stresses are caused in the bond line which normally increase the stress peaks at the extremities of the bond line significantly and lead to a considerable decrease of the transferable external force, see Figure 2.

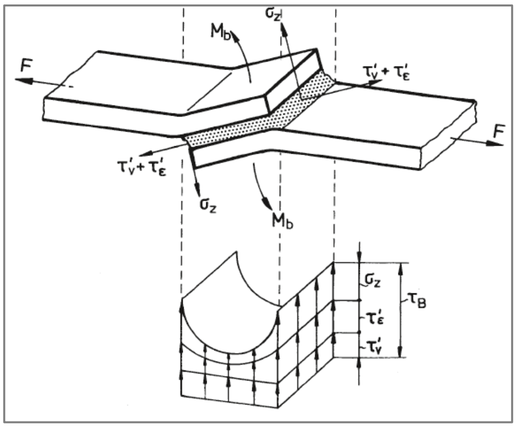

Figure 2: Principle of full stress distribution in a SLS application considering shear and peel, Ref. 6.

In order to reduce these stress peaks and to increase the strength of the joint, several ideas emerged in the past, see Ref. 3, Ref. 4, and Ref. 5 as examples. All these efforts focused on reducing the stress peaks only but did not improve the damage tolerance behavior in the bond line itself. As a consequence, in aerospace applications the authorities always pay special attention to this type of structural joint.

On top of these examples, there is other work about influencing the stress-state of structural bondings (as for example with gradient adhesives) but according to the knowledge of the authors none of them is focusing on a full arresting feature in the bond line by a design feature regardless of stress state or load direction.

3.2. Design principle for a lap shear joint with damage tolerant characteristic

The most effective strategy to improve the damage-tolerance behavior of a bond line is to establish reliable features for stopping a potential growing crack in the adhesive. Examples are given and examined in Ref. 7. A very reliable means to arrest a crack is a free edge as by definition all growing cracks stop at a free edge of a part. Based upon this cognition, for the newly developed design principle a separation of the bond line along its running length into a plurality of simple shaped sub-bonds is proposed. The result of this is a purely geometrical modification of the constant overlap length along the lap-shear splice joint by an intermeshing pattern of the panel's ends, see Figure 3.

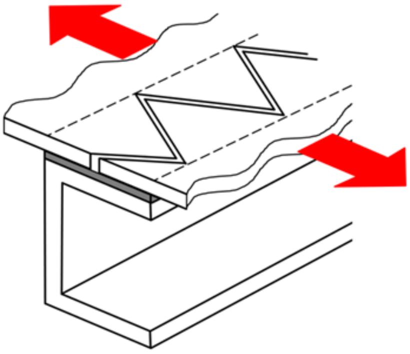

Figure 3: Principle of the sub-division of the bond-line along its length.

In combination with the splice-plate underneath (which is a frame or longeron in the real structure), this intermeshing pattern creates as example a zig-zag bond line which generates a plurality of separated sub-bonds. From a global perspective these sub-bonds act together as one single bond line but transfer the corresponding running load of the complete bond line individually. In case one sub-bond fails, the local loads are taken by the adjacent sub-bondings. In this way the global load transfer is ensured as far as this scenario is covered by the substantiation of the bond line (i. e., the failure is simulated and the additional stresses are taken into account in the sizing).

As stated before, the most important function of the intermeshing zig-zag-line is to completely separate the individual (here triangular) sub-bondings. But due to the shape of the zig-zag pattern the state of stress is impacted as the fluxes are no longer constant along the running length in case of an applied tensile load, see Figure 4.

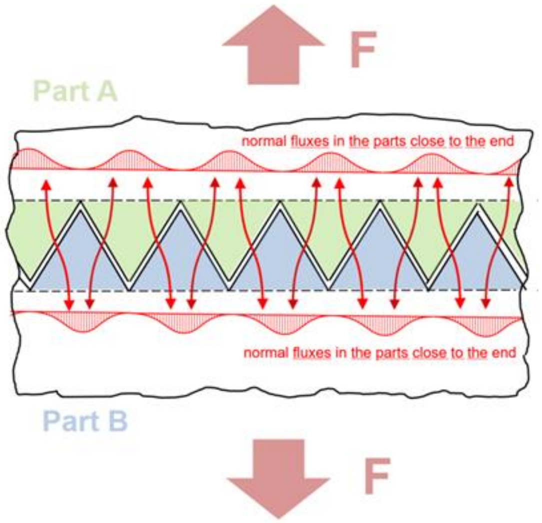

Figure 4: Stresses / fluxes in the parts in top view.

It becomes clear immediately that the standard equations from Ref. 1 or Ref. 2 are no longer valid for the description of the stresses as for example there is no more constant overlap length along the bond line. This means that the peel stresses as well as the shear stresses are varying along the length of the bond line. In order to ensure that the stresses in the bonding are kept well below the allowable strength of the adhesive in shear and peel, detailed examinations of the stress state have to be performed.

3.3. Geometrical parameters influencing the stress state

Basic examinations about how the new pattern influences the stress-state in general showed that the triangular pattern of the intersection line has the positive effect on both, peel and shear stress in the adhesive, see Ref. 8. In this previous publication a big number of influencing geometric parameters on the sensitive stress state are described in detail. In brief, it can be stated that the separation of the bond-line into a pluralty of triangular sub-bondings has a significant stress reducing effect as the utilization factor of the adhesive is increased. The stress peaks in shear and peel are reduced by about 15% – 30% (dependent on the adhesive and some other influencing parameters such as thickness of the bonding and the bonded parts).

It was found that compared to the classical lap-shear joint all stresses are lower by using the new intersection pattern. In Ref. 8 this general beneficial behavior is verified by tests for different paste adhesives.

The following figure highlights the reference shape for all parameter studies carried out on the new design feature.

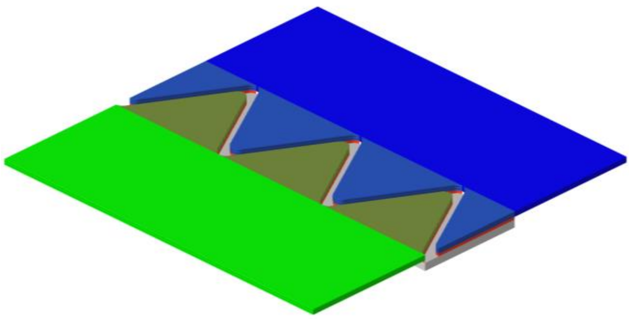

Figure 5: Basic geometry of the new bond line pattern: a triangular intermeshing zig-zag line of both panel ends.

This basic shape is simple to manufacture and offers to be a reasonable option for the implementation in a real aircraft panel. As well all examinations in Ref. 8 were based upon this triangular shape of the intersection line. For the time being it is still not clear if the triangular shape is the best shape of the intersection line between the panels. Much more patterns are feasible beyond the ones shown above and have to be examined with respect to their influence on the stress state. This is not performed now but will be subject of future research work. For the time being the triangular shape is chosen as a reference geometry for the research work shown in this publication.

The stresses in the adhesive are key for the load transfer and thus they were examined thoroughly. In Figure 6 the stresses in the adhesive are plotted for different patterns of the intersection line: At first the stresses in the adhesive of a triangular patten as reference geometry, then the same stresses in a sinusoidal shape and finally in a trapezoidal shaped intersection line. All of these patterns have the same area as basis for comparison. It can be seen clearly that the shape has a strong influence and that amongst the shapes shown in this figure the triangular shape seems to be the geometry offering the lowest general stress level amongst these patterns. Note that the scaling on the plots is set to the identical stress levels.

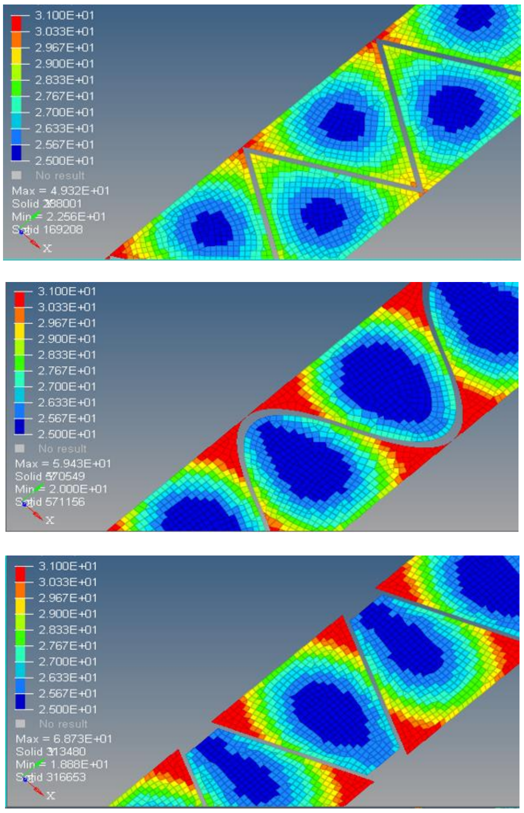

Figure 6: Stresses in the adhesive for different shapes of the bond line.

3.4. Additional parameters influencing the stress state in the adhesive

As in the common single-lap shear bonded joints there is a big variety of parameters which have a partly huge influence on the stress-state in the bonding. These parameters are for example the thickness of the panels, the adhesive itself of course (mainly its Young's modulus or shear modulus), the thickness of the adhesive, temperature, humidity, and manufacturing tolerances. In the first basic examinations, the majority of these parameters were examined and already published in Ref. 8. In that publication all parameter studies were based upon the triangular shape of the sub-bondings as well. It was found that most of the manufacturing tolerances had a low sensitivity or – in case there is a big influence – the manufacturing aspect in tendency had a positive impact on the stresses as the stress peaks were decreased. As an example: in case adhesive material is pressed out of the contact areas between the panels and splice-plate, it accumulates in the free gap formed by the zig-zag line and the splice plate. And if this gap is filled with excessive adhesive material accordingly, the stress peaks go down significantly. This is identical for excessive adhesive material which is pressed out at either end of the splice plate during the compaction process in manufacturing: the additional adhesive offers additional cross-section for load transfer and moreover reduces the local stress peaks due to a reduction of the notch effect (see for example Figure *6*).

During the numerical examinations it turned out that if the nominal theoretical geometry (without manufacturing tolerances, precise conditions and no stress reducing effects like excessive adhesive which is pressed put anywhere is taken as basis for the stress calculations, this is the worst case condition covering the others scenarios with manufacturing tolerances.

4. Detailed FE-calculations

4.1. Scope

In order to support a future certification of a joint using the new design principle a reliable data basis about the stress state in a bond line with the new design principle has to be generated. This was performed based upon dedicated FE-studies in the frame of the research project. In co-operation with specialized research partners and institutes at universities dedicated high-fidelity models of the new design principle were established. These were calibrated with measured material data from coupon tests in order to get a deeper insight into the stress state including the effect of an impact damage. Additional goals were to evaluate the functionality of the elaborated design principle with respect to:

1) examine if possible cracks stay in the adhesive and do not grow into the substrate at any time,
2) evaluate residual strength of the bond line under the assumption of an artificial damage in the area of the bond line (BVID or local disbond),
3) predict the direction and speed of the crack growth within one triangular sub-bonding and to compare it to a common configuration.

4.2. Calibration of the high-fidelity models

A big variety of calculations was performed during the research work and on top a set of different FE -models were established in order to examine specific effects. All models have been "calibrated" in order to show the best fit between the simulations and the coupon tests (see paragraph 5.2). For this the configuration of the test was re-built in an FE-model and the parameters of the adhesive as well as its interface to the joined components were tuned in order to achieve the best fit of the measured strain-displacement curve, see Figure 7.

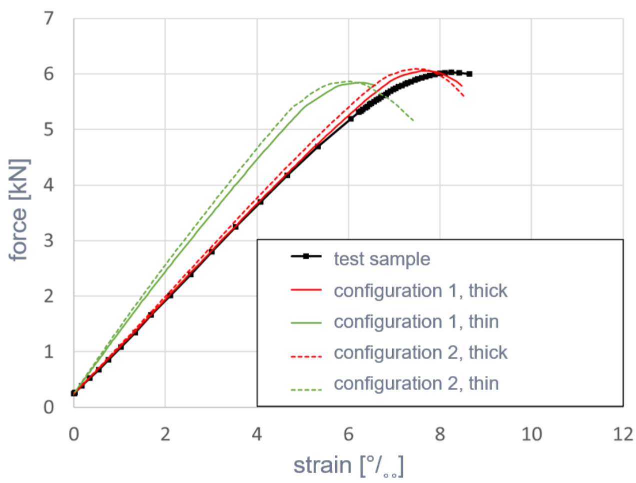

Figure 7: Example for the calibration of the FE-models to fit the strain-force curves of the samples. The red parameter set was chosen finally.

In this figure, as example, the adaption for one sample type is shown where for one stacking sequence of the panels several ABAQUS-parameters were adapted and different adhesive thicknesses were checked. The set of parameters shown in the red curves were chosen finally as they showed the best overall fit between test and FE-model.

In order to increase precision, the models for the common rectangular shape and for the new triangular shape were calibrated separately. In this framework several publications about the description and calibration of the FE-models used for the examinations work were published (Ref. 9, 10, 11). They have to be consulted for details as the publication at hand focusses on the application of the new bonding principle.

4.3. Examination of the crack growth

Although the basic idea of the new bond line design is to stop a possible crack growth at the limits of one sub-bonding completely, a study was carried out regarding the crack propagation within one sub-bonding. The main reason was to learn about the velocity of crack propagation in comparison to a classical bond-line as the stress-state is significantly different, see previous paragraphs.

The detailed analyses presented here are based upon a dedicated FE-based crack propagation model using cohesive-zone elements. One limit is that the set-up of the model does not allow to predict the number of cycles required till crack initiation. Thus, at the beginning of the computation the initiating crack position is to be chosen artificially and then the real crack propagation starts. The location of the crack initiation was done by selecting the spot with the highest peak stress in the adhesive in a simple static analysis.

On top, the crack propagation model calculates the static damage according to the traction-separation-law and thus at the end of the simulation the sample fails suddenly by exceeding the remaining static strength of the adhesive. The material data used for the adhesive for the Paris-law of the accumulated damage were calibrated to match the results from the fatigue tests carried out on coupon level, see paragraph 5.2.

In a first loop, the numerical module calculates the crack propagation in one isolated strip of the complete bond-line representing the width of one triangular element, see Figure 8. Red areas in the figure highlight the complete loss of adhesive strength (adhesive failure).

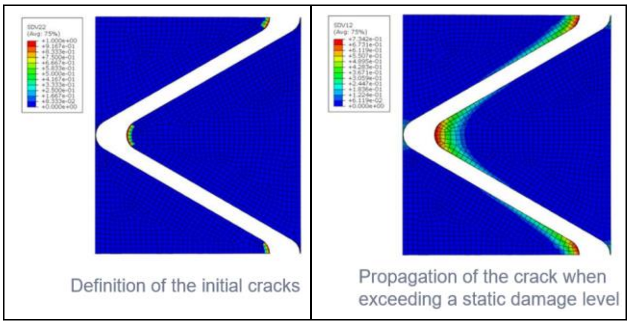

Figure 8: Simulation of crack propagation in one triangular element: definition of the initial crack (left) and typical crack propagation (right).

In the simulations on this level, three spots for crack initiation were chosen at the same time as at all of these locations the stresses were on identical level due to the symmetry of the model. So, each tip of the triangle is prone for crack initiation. With increasing cycles, the cracks are propagating with increasing speed as the remaining functional area of the adhesive is decreasing with crack propagation. The figure below shows the time history of the crack growth: the red and green line show the mean position of the crack at a propagation from either side of the joint. The blue dots in the graph on the righthand side of Figure 9 depict the full propagation of the crack tip until failure which is around 250`000 cycles after initiation. Then the sub-bonding fails completely considering a constant load level acting on the adhesive. This is not valid in a practical application as the global loading is shared by the remaining sub-bondings which are still completely intact. Thus, in reality the crack growth would happen with lower speed.

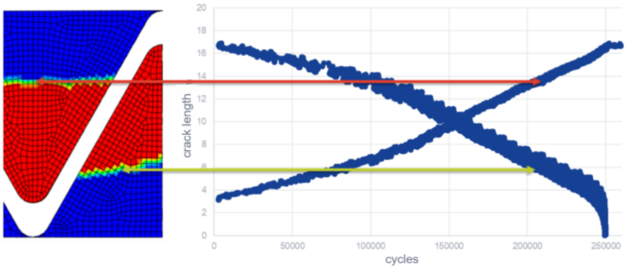

Figure 9: Crack length over cycles. Red area represents a failed adhesive, blue represents intact bonding.

Having verified the crack propagation on the level of an isolated triangular element, a bigger model was put together by joining 5 triangular sub-bondings to a wider specimen. This is to simulate the crack propagation considering a load share between several triangular elements. It is important to emphasize that the crack in the triangular specimen stops at the limit of one triangle whereas in the regular bond line the crack grows without being stopped. In Figure 10 for one of the adhesive materials a comparison of the crack propagation is shown: The yellow triangle which is limited by the red line represents a crack in a regular wide single lap shear configuration where an artificial crack growth in the adhesive is initiated in the area of the gap between both panels (or around the middle of the splice plates respectively).

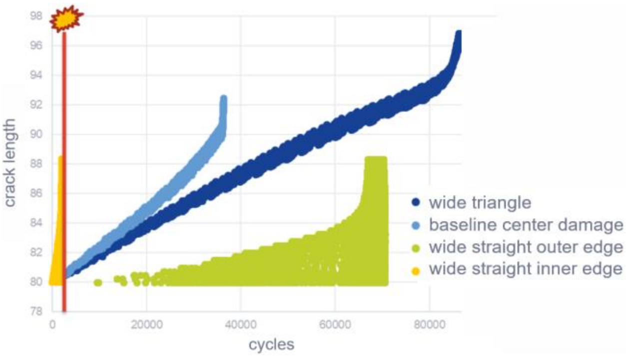

Figure 10: Crack propagation in different configurations of a wide specimen configurations: wide triangle, wide regular with different damage locations.

The crack grows quickly along the running length of the lap joint and fails in this simulation at about 2000 cycles. In case the crack is initiating at the outer ends of the splice-plate, the crack growth is much slower and fails around 70’000 cycles in case the same load level is applied. In contrast, the specimen consisting of 5 triangular sub-elements (dark blue curve) lasts about 85`000 cycles until the damaged triangle is lost completely. Then the crack stops by definition at the extremes of the triangle. In the simulations the crack is arrested afterwards as there is no contact between the triangles. But there is still no complete failure of the joint (as it was calculated in the regular configuration) because the remaining triangle are still capable to transfer the applied load. So, at 85`000 cycles the crack is stopped but the specimen is globally intact.

Even in case the simulations consider the gap is filled with adhesive completely, the calculations showed that the crack does not propagate into the adjacent un-damaged triangles. This is a good indication for the robustness of the new principle as even in case the sub-bondings are connected by adhesive (as it would be in a real manufactured joint), the crack growth would be stopped according to the models.

Main result of the numerical simulations is that the velocity of crack propagation is significantly lower than in a classical bond line and stops before the complete failure. This is an additional beneficial behavior of the new principle: in case cracks are occurring in the bond, the propagation is much slower than in classical bonds. This means that the time required to disrupt the complete load transfer on one sub-bonding is up to 40 times longer than in a bond without this feature (dependent on the adhesive of course).

4.4. Determination of strength and deformation

The derived calibrated FE-models were used for several purposes:

- Verify the results generated based upon the comparatively coarse engineering FE-models.
- Verify that all local effects are addressed in the simplified models.
- Predict the effect of several parameters such as manufacturing tolerances, impact damage, and residual strength.
- Support the evaluation of the tests on coupon and detail level with respect to the local effects initiating the failure of the joint.

With these models a very precise description of the expected failure load for different configurations was possible. In addition, already known principal effects such like the positive effect of a 45° orientation of the CFRP layer at the interface to the adhesive could be verified, see Figure 11.

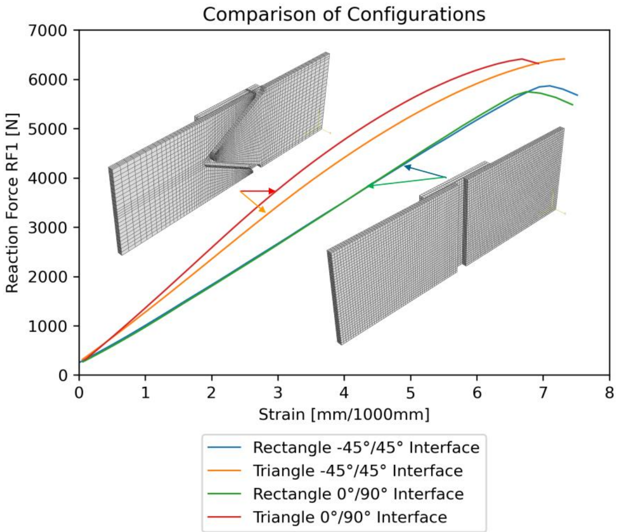

Figure 11: prediction of different configurations: rectangular and triangular with different orientation of the layer at the interface to the adhesive.

An important step was to verify the increased load transfer capability of the new principle. One of these effects is the significantly decreased out-of-plane deformation of the triangular shape as with increased overlap length the detrimental peel stresses in the adhesive are reduced significantly. This is shown in Figure 12 where the out-of-plane deformation under tension load is given: The blue and green dots show this elastic movement for two different lay-ups for the common shape whilst the orange and red dots show this for the new triangular shape at the same load. An important detail can be seen as well: in the common rectangular shape a certain-dis-continuity of the out-of-plane movement can be seen just in the middle of the joint (at the gap location). This indicates singularities in peel stress. Comparing this to the much smoother and lower displacement curve of the triangular specimen, it can be concluded that the peel stresses are significantly lower and spread to a wider area in the specimen with triangular bonding.

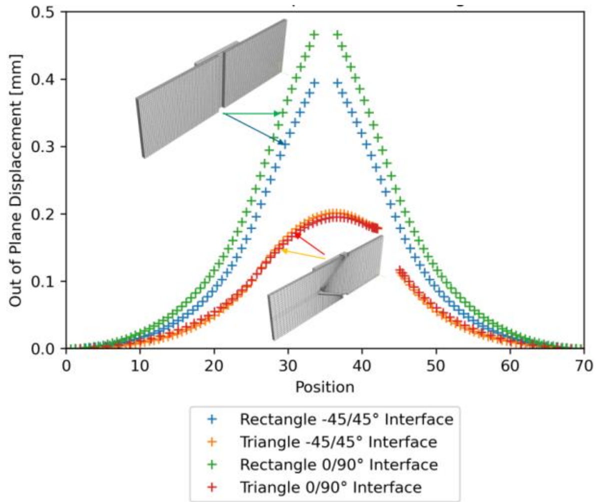

Figure 12: prediction of the out-of-plane displacement of a common rectangular configuration and the new triangular shape.

Finally, the high-fidelity models gave high confidence during the research work that all influencing parameters on the strength and failure behavior of the new principle have been understood. With this a reliable basis is given for a simplified, enveloping sizing and substantiation method which is conservative and does not require the use of the high-fidelity models any more (see chapter 6).

5. Test campaign

5.1. Test strategy

One of the main goals of the research work was to establish a basis for the certification of damage tolerant structural bondings in aerospace applications. The certification aspect implies that besides thorough theoretical assessments (see previous chapters) the principle has to be validated by test. As a completely new design principle was defined, the test campaign started at the bottom end of the test pyramid: tests on coupon level in order to characterize the basic functional principle and then on detail level for the verification of the mechanism for damage tolerance in a realistic panel.

5.2. Tests on coupon level

On this level two different main questions were answered: At first to verify the positive impact of the triangular shape on the stress state in the connection and second to characterize different adhesives, layups, conditions, and impact of typical damages on the static and fatigue strength of the new bond line design. As secondary effect, the test results can be used to calibrate the numerical results (see chapter 4) in order to increase precision of the calculations.

The specimen on coupon level were single lap-shear joints. Two substrates made of 5 plies of bi-directional CFRP fabric were bonded to an aluminum strap. The overlap length is 20 mm, the width is 23 mm in order to accommodate one complete triangle in width, see Figure *13* lower area. As reference configuration a common lap shear joint with rectangular shape was tested as well, see Figure *13* middle area.

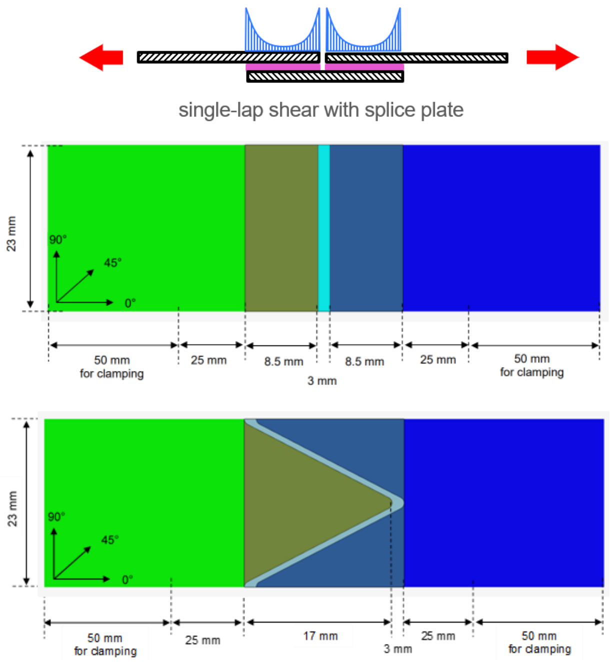

Figure 13: Single lap shear specimen for the coupon test campaign. Upper: cross-section with applied load. Middle: rectangular specimen as reference. Lower: triangular shape with identical bonding surface.

All coupons were loaded in pure tension till rupture. The areas of the bonding for both types of specimen were identical so that the nominal shear stress (force divided by area) can be compared without any size effect.

As the campaign on coupon level was already subject of a previous publication (see Ref. 8), only the main results are summarized here. Figure 14Figure *12* shows the impact of the new triangular intersection line on the strength of the bonding. For three different adhesives (*Scotch-Weld 9323 B/A* (orange), *Hysol EA 9395 A/B* (blue), and *Aeropaste 1006* (yellow)) static strength tests were carried out. The only difference in the tests is the shape while the bonding surface area of both configurations was of identical size in order to be comparable. The figure highlights that the strength of the new intermeshing pattern increases strength between 12% and 30% dependent on the used adhesive. This is in line with the result of the numerical examinations which showed a decreased stress level in the adhesive with the new triangular pattern (see paragraphs 3.3 or 4.4 and especially Figure *11*). It becomes obvious that the strength increase is caused by the new triangular pattern but is influenced by the type of adhesive.

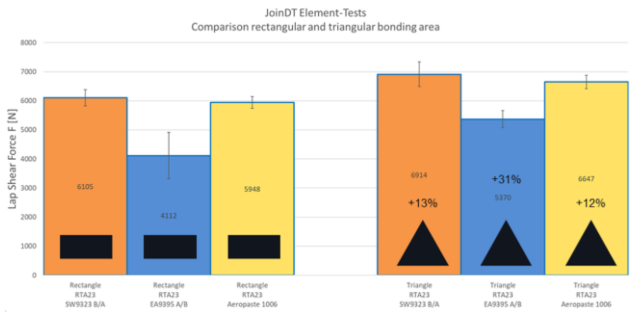

Figure 14: Overview of the static strength increase of the new pattern for different adhesives. Left side: strength for typical straight intersection line. Right side: strength for the new triangular pattern.

The influence of the environmental conditions is shown in Figure 15. On the left side the strength at room temperature and ambient conditions is shown and on the right hand side the influence of a hot and wet environment: Dependent on the type of adhesive the environmental effect is significant and needs to be considered in the sizing and substantiation. This is an effect which is independent of the shape of the bond line but a pure characteristic property of the adhesive itself.

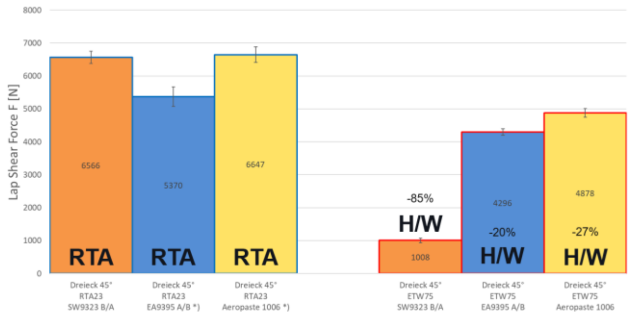

Figure 15: Influence of different environmental conditions on three different adhesives. Left side: room temperature and ambient condition. Right side: Aged specimen in hot / wet environment.

Another study on coupon level was performed to examine the effect of certain defects in the bond line. Different tests have been carried out in order to study different types of damages compared to a non-damaged specimen on the new triangular configuration, see Figure 16. The pristine baseline configuration is shown on the left side in this figure. The second set of columns shows the specimen`s strength with a typical impact damage put on the triangle (BVID, similar to the ones on detail level, paragraph 5.3). It becomes visible that dependent on the adhesive there is a dramatic drop of the strength after impact (*Hysol EA 9395 A/B*) while for the others there is very limited sensitivity (*Scotch-Weld 9323 B/A* and *Aeropaste 1006*).

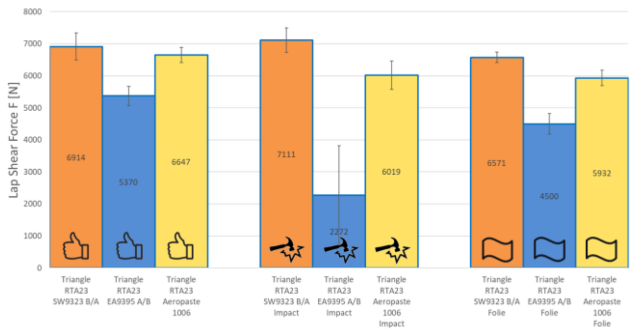

Figure 16: Influence of typical damages (BVID and local dis-bond) on the static strength of the new principle for three different adhesives

Considering a local dis-bond at the tip of a triangle shows a low impact on strength as depicted on the righthand side in this figure: when a thin Teflon-foil was introduced at the tip of the triangle which covers about 30% of the overlap length of the triangle, there is a very limited drop in. This is independent on the type of adhesive. This behavior is similar as in the simulations where the stress increase was very low due to the locally removed adhesive.

Result of the coupon tests: In summary the coupon results showed very encouraging results. In comparison to the standard shape the increased strength was confirmed and an in-sensitivity to damages is noticeable. The impact of environmental conditions is related to the adhesive only and is not dependent on the shape at it is a pure material parameter.

All in all, the coupon tests showed a superior behavior of the triangular shape compared to the common rectangular shape and no indication for a detrimental behavior was found.

5.3. Tests on detail level

The main goal of the tests carried out on detail level was to prove the principle of damage tolerance in case of a partially failed bond line for any reason (local dis-bond, BVID, crack, etc). As in a real panel the loads are running loads which are shared by all triangular sub-bondings equally. In this configuration the individual sub-bondings are not loaded in a force-driven manner separately but they act as one complete junction where the individual sub-bondings are rather loaded in a displacement-controlled way because the global stiffness is limiting the displacement in case there is one “failed” triangle.

In order to have a good transferability to a real bonded panel in an aircraft, the typical lay-up in a typical configuration used at Airbus Helicopters was chosen as baseline: a sandwich panel with 3 woven CFRP fabric plies outer skin and 2 plies inner skin, getting together to 5 plies in the monolithic area of the bonding joint. The chosen size of the panel incorporates a “big number” of triangular elements, so that in case of a failed sub-bonding “many” remaining triangular elements are left in order to take the loads of the failed bonding, see as well chapter 6 for details. Based upon this the configuration as presented in Figure 17 was chosen: Test specimens with respectively two ca. 500 x 500 mm sandwich panels joined together in the middle by a zig-zag intermeshing line on a center frame flange acting as splice plate.

Two separate test campaigns were carried out during the research project: Pure tension of the two joined panels, to see in the upper part of Figure 17 and combined shear/bending caused by a lateral load, to see in the lower part of Figure 17.

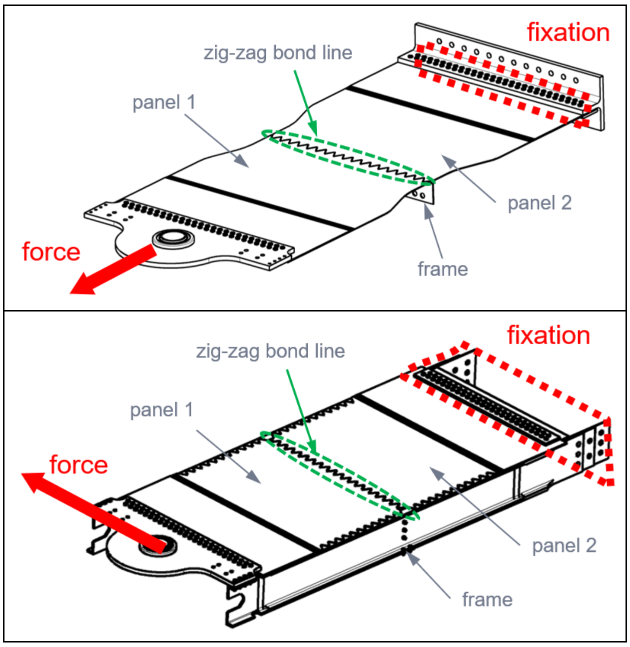

Figure 17: Principal arrangement of the two panels for the tensional tests (upper) and bending/shear tests (lower).

Tension tests: performed in order to characterize the tension strength of the chosen panel / frame configuration:

1) Specimen 1, having a BVID on one triangle to investigate possible crack propagation. First tested statically to LL and UL, then tested in a second step under cyclic loading with 0.7 x LL at R = 0.1 for 10^5 cycles. Afterwards again loaded statically to UL and then to rupture in order to show residual strength with impact damage after cyclic loading.
2) Specimen 2, having one triangular sub-bonding removed from the bond line ("artificial damage") in order to simulate one failed sub-bonding. Also tested first statically to LL and UL, then under cyclic loading with 0.7 x LL at R = 0.1 for 10^5 cycles. Afterwards again loaded statically to UL and then to rupture in order to show residual strength with impact damage after cyclic loading.
3) Specimen 3, having two additional triangular elements adjacent to the first one removed in order to simulate that a damage might have destroyed several adjacent triangles.
In further steps, and always after UL applied statically, more and more triangular elements were removed out of the load path until final failure of the specimen.

Limit load (LL) was here defined as the loading where the outer sandwich skin of the panel under the chosen condition reaches a value of 3000 µstrain, at Airbus Helicopters a standard sizing principle for a damage tolerant CFRP structure (UL = LL x 1.5).

Combined shear/bending tests: in a more complex loading condition the bonded joint was characterized under static loading as well in the same way as the tension specimens:

4) Specimen 4, having a BVID on one triangle. First tested statically to rupture in order to identify max. load capability under this loading condition.
5) Specimen 5, having one triangular sub-bonding removed from the bond line ("artificial damage") in order to simulate one failed sub-bonding. Also tested first statically to LL, then under cyclic loading with 0.7 x LL at R = 0.1 for 10^5 cycles. Afterwards loaded statically to UL and finally to rupture.
6) Specimen 6, having two additional triangular elements adjacent to the first one removed in order to simulate that a damage might have destroyed several adjacent triangles.
In further steps, and always after UL applied statically, more and more triangular elements were removed out of the load path until final failure of the specimen.

The last configuration (6) was tested in static loading conditions only as this is a very severe configuration which represents a situation where for example a damage after cyclic loading would have destroyed more than one sub-bonding or where a crack theoretically grew over the limits of one triangle (which is not possible based upon the current knowledge of the new principle). This procedure saves time as the result of the crack growth is simulated (=failed sub-bonding).

In Figure 18 the impact damage is shown which was applied on one of the triangular sub-bondings. As there is an aluminum frame flange underneath, the impact energy caused a significant remaining deformation on the surface.

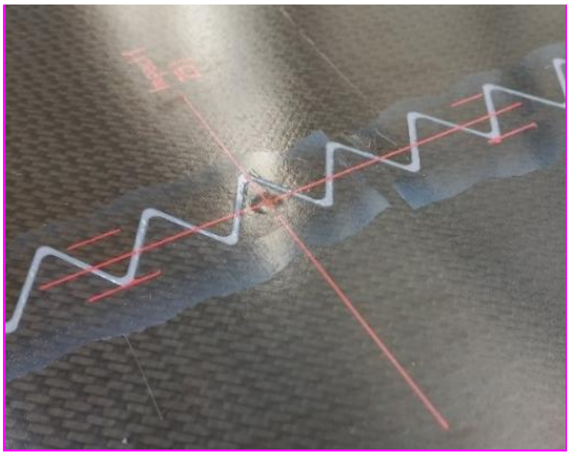

Figure 18: impact damage on one triangular sub-bonding. The remaining damage is clearly visible.

An impression of the artificial damage in a bond-line is given in Figure 19. The red lines show the position of the cut line for the “removal” of one triangular element from the bond line, the white line in between depicts the through-thickness cut at the foot of a triangle. At this line this sub-bonding is set to in-active by complete separation from the load path.

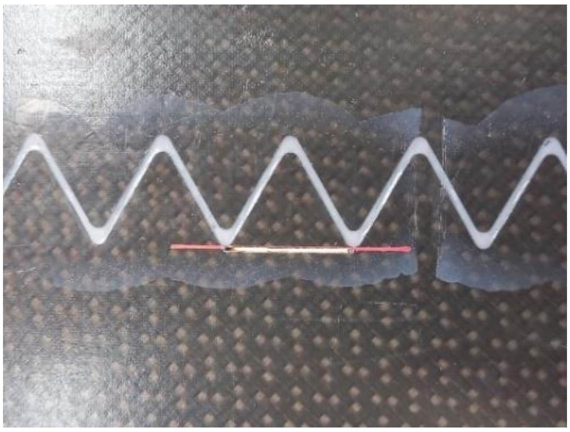

Figure 19: artificial damage introduced on the bond-line: through-thickness cut in the panel in order to remove one triangle from the load path. The white line represents the cut.

In a late phase of detail testing (step 6 in the test sequence listed above) several elements were removed by extending the cut line triangle by triangle.

Important note: The assumption that a crack is growing from the BVID or artificial damage and enters into the next triangles is purely theoretical as this was not observed during the test campaign. This was a conservative assessment only in order to test an extremely worst-case condition where a damage extends for a theoretical reason to a growing number of triangles.

5.4. Results of the element tests

Tension tests: The specimens loaded in tension showed no sensitivity to the fatigue cyclic loading or to any of the damages introduced to the bond line (BVID or removed triangle). In both cases (No. 1 &2) UL level was applied to the specimen after being loaded in fatigue. After the application of UL both specimens reached the identical failure load which was about 9% higher than UL. Both specimens showed the identical failure mode which is shown in Figure 20.

Ultrasonic inspections of the bond line were performed before and after the application of the cyclic loads and did not indicate any crack growth or degradation of the bond line, in special not tin the area of the BVID or in the vicinity of the cut triangle.

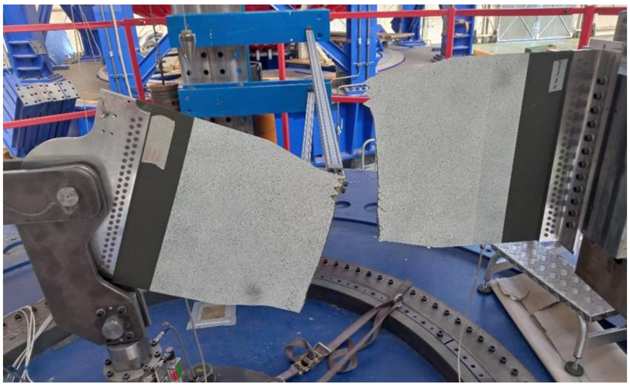

Figure 20: tensional loaded panel after rupture

The final rupture of the specimen’s bond line was caused by cohesive failure of a fraction of the bond line as a sudden failure. This then led to a rupture next to the bond line in the panel laminate. Thus, the limit in strength is caused by the strength of the adhesive itself which is the design point.

Tests in combined bending/shear: The specimen in these tests had a more complex loading condition as in-plane-bending and shear are put in superposition. This causes on the compression side an elastic out-of-plane movement of the panel which was considered to be significant. This out-of-plane movement is caused by the offset in the neutral fiber of the honeycomb panel under compression and was not explicitly looked at in the analyses. During conduction of the first test, it was recognized and taken into account accordingly. As this secondary elastic movement is highest in the monolithic area of the panels close to the vertical zig-zag line, it was difficult to rate the impact on the local bonding strength. Reason is that the computational models did not take this non-linear effect into account and as consequence the additional peel introduced in the bond line locally was not taken into account. It is to be noted that the sensitivity of lap-shear joints to out-of-plane stresses is known to be significant.

Both tested panels showed the same failure mode as it is shown in Figure 21: The panel on the load introduction side separated completely from the surrounding framework with the observation of a primarily cohesive failure at the triangular bondings. Noticeable was an additional diagonal crack on this panel (shown in the lower left corner in Figure 21) but it was not possible to detect if this crack was the initiation of the complete failure or if the failure at the bond line caused this damage. Further examinations have to be carried out.

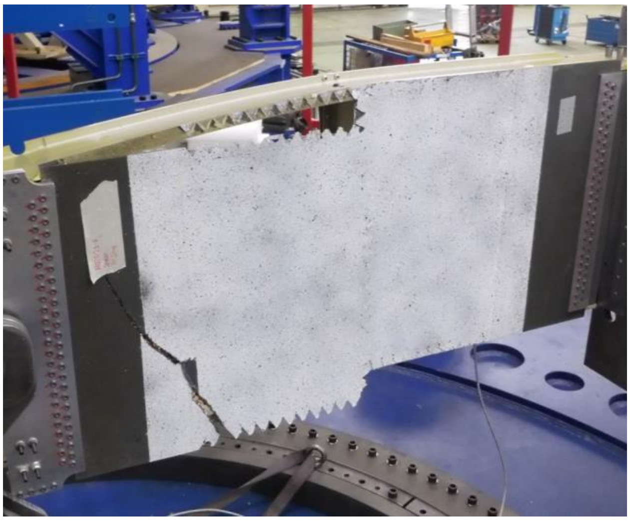

Figure 21: panel loaded in shear/bending after rupture. Load application on left side in downward direction.

The first sample with pure BVID impact damage (test sequence No. 4 in the listing above) was tested to a load level until failure in order to determine the rupture strength including the unknown peel stresses which were described above. Based upon these corrected panel strains a lower load level had to be defined as LL and taken as basis for the 0.7 * LL for the cyclic test of the second specimen.

In these tests as well, the bond-line was subjected to ultrasonic inspection before and after the application of the cyclic loads and no indication was found for any degradation or crack propagation. After the cyclic tests the specimen was tested up to rupture (see Figure 21) in accordance with the test sequence described above.

Last step was to test the robustness of the junction (test sequence No. 6 in the description above). Although a propagation of a damage or crack was never observed in any of the tests and neither found in the simulations, several triangles were removed step by step during the tests. With each additional removed triangle the specimen was loaded up to UL. After the stepwise removal of 14 adjacent triangles the specimen failed as shown in Figure 22. The green bracket in this picture highlights the area of the cut triangular sub-bondings. Note that almost one third of the complete bond line had to be removed before the connection failed. This demonstrates an extreme robustness not only at tension but at this loading condition as well.

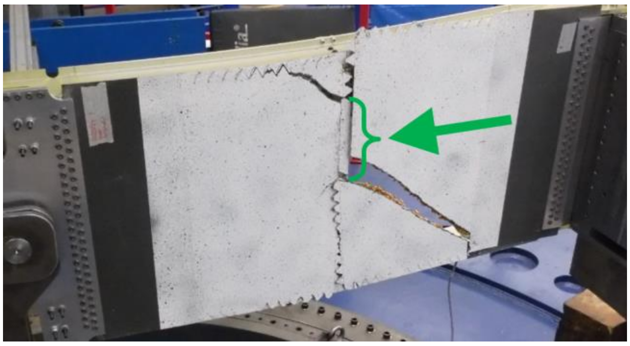

Figure 22: panel with several adjacent sub-bondings cut (green area). Status shown after rupture in bending/shear load application above UL.

As the broken panel looks slightly different compared to the previous ones (mainly the secondary crack described above) a direct comparison of the failure mode to the one under tension is difficult. According to the indications after dis-assembly it can be stated that the failure in the bonding was mainly cohesive failure again.

In both configurations, pure tension and combined bending/shear, taking into account the differences between the specimen (BVID versus removed sub-bonding) it can be stated that the load transfer principle is very robust and one “failed” triangle does not impact the strength of the bond line significantly. As a consequence, in a real bonded structure an un-detected damage can be accepted without special consideration in the substantiation in case a sufficient number of triangles is put in place.

6. Preliminary design principle and sizing rule

According to the detailed FE-examinations and the matching test results it can be stated that the new design principle is enveloped by the well-established equations for common lap-shear joints. This simplifies the substantiation significantly because no optimization is to be performed for the new principle. In consequence the margins of the bonding will be higher than calculated based upon the common lap-shear allowables. Anyway, several general rules have to be respected in order to be covered by the examinations performed till now.

First step is to ensure that the design principle is properly applied from a geometric point of view. Then a reasonable geometry (triangular shape) with reasonable size has to be chosen. As the research work focused on a triangular shape of the intersection line, no scaling factors for other geometrical shapes are available at the time and in consequence a similar pattern should be used for practical use unless more geometries are examined.

Intentionally the basic geometric data chosen for the simulations and tests were based upon the typical frame to skin joints used in the Airbus Helicopter fleet: The width of the frame flange was taken over from the areas where two panels have to be joined together at this frame position. With this the manufacturing and assembly tolerances of the related panels and frame position are already verified. A reasonable pattern is found by the definition of the simplest shape of the individual sub-bondings: An isosceles triangle which is intermeshing from both panel sides. With this design rule a reasonable size and shape of the intermeshing pattern is given as starting point and shall be taken as basis for the sizing and substantiation of the bond line.

The strategy in developing a practical sizing rule for the new type of structural bonding is not to establish an extremely detailed level of calculations as for example described in the previous paragraphs. Excessively detailed calculations based upon fine meshed FE-models would be expensive and time consuming and hinder the use of the design principle in possible fields of application.

Thus, an extremely simple approach was made: As a general goal in aerospace applications the weak point in joining structural elements should never be the joint itself but the surrounding area of joining parts. So, the strategy is to take the sizing criterion of the panels (nowadays made out of CFRP) which is based upon a strain-criterion in order to show no-growth of BVIDs in CFRP under the repeated loads.

Driven by the static needs in a typical frame-to-skin joint and related manufacturing limitations, structural bondings can normally transfer very high static loads. The tests performed showed that the forces occurring in real structures will never reach the static limit of the joint in practical application. As highlighted above, all examinations proved that the transferrable load in the new design is higher compared to a classical design and so it is conservative to use the standard equations for bonded joints as described in Ref. 1 and Ref. 2. In case this approach is too conservative, a simple scaling factor can be used in order to get closer to the real strength of the joint if required.

As demonstrated and thus per design principle a potential crack cannot grow bigger than the size of one triangular sub-bonding. Therefore, a crack propagation analysis is not required: The sizing of the bond line is done by considering that two or three adjacent sub-bondings can fail without significant impact on the structural strength of the entire joint. For this in a first step the bonding is considered as continuous bond line in order to identify the locations with the highest stresses in the bond line. At this location two or three sub-bondings have to be removed from the bond-line and with this configuration the bonding is sized again using the common equations for regular SLS bondings. Possibly the overlap length has to be increased locally or the size of the sub-bondings has to be decreased in order to reduce the local effect of the failed sub-bondings.

Fatigue calculations are not necessary as there is no benefit to know how many cycles a possible crack needs to propagate till the borders of the sub-bonding because in theory this part (or two) was already considered as “removed” or “failed” respectively (which is conservative). As the crack is stopped effectively the crack doesn’t start in the adjacent un-damaged sub-bondings and thus fatigue is basically covered by the initial static sizing implicitly.

This substantiation strategy is similar to the sizing philosophy of bolted joints in fatigue sensitive applications. In this case, it is assumed that one (or two) fasteners can fail and with the remaining intact fasteners the connection can still transfer LL. Now in an analogous strategy one sub-bonding is considered as discrete (fastener) element which transfers a fraction of the total load similar to one fastener.

Figure 23 gives an impression of the similarity when comparing it on global bond line level: The black points indicate typical positions of fastener positions in case two panels are riveted together in a staggered manner. The triangles are representing the same staggered configuration but are simply replacing fasteners by sub-bondings.

The fact that bolted joints are also sized for inter-rivet buckling of the sheet can be neglected here completely. This means that actually one failure mode less needs to be addressed and thus less sub-bondings may become necessary than fasteners originally.

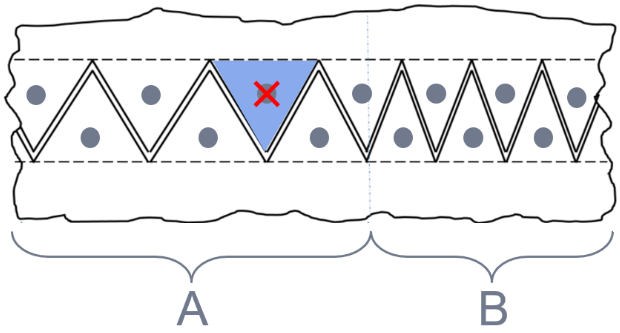

Figure 23: Top view of an intermeshing bond line pattern. The width of the triangular sub-bondings is different in area A and B and the points represent bolt positions in case of a bolted joint connection (as analogy).

Currently the substantiation principle for bolted joints is to remove one bolt for proving fail-safe behavior or damage tolerance respectively. This is shown by the bolt marked with a red cross in Figure 23. In case of a bond-line the load transfer is impacted locally in case one triangular sub-bonding has failed (blue triangle in this figure). In both cases, a row of fasteners and the plurality of sub-bondings, the adjacent elements have to take the load from the failed item and in both cases the local flaw which caused the failure cannot propagate to the next joining element. So the behavior between both joining principles can be considered as being similar in this aspect.

On top, in case the sizing process described above unveils a high sensitivity when removing one or two triangles, the size or density of the triangular sub-bondings can be adapted as shown in Figure 23: In areas of low failure sensitivity (zone A in this figure) the size of the triangles is bigger than in areas with high failure sensitivity (zone B). This is analogous to introducing more fasteners per length in a bolted joint connection.

7. Current status and future work

All results generated during this research support the functionality of the principle to effectively stop a possible crack growth in a bond line by the separation into multiple sub-bondings. In the numerical examinations as well as in tests no indication was found that the developed design principle with intermeshing zig-zag line of the joined panels is not working effectively and at least covered by the classical lap-shear joint principle.

The tests performed during the test campaign revealed that the standard adhesives *Scotch-Weld 9323 B/A* and *Hysol EA 9395 A/B* are not applicable in a real application. For the time being the most promising adhesive is the *AeroPaste 1006* adhesive which is currently in qualification at Airbus.

For sure, a suitable adhesive is key for a successful implementation of the new design principle but in fact, the basic design principle described in this publication is not dependent on the type of adhesive or even if it is a bond line because this principle can be transferred identically e. g. to welding of thermoplastic panels.

The key question and starting point of all work is the behavior under repeated loads and if or how possible imperfections lead to cracks and propagate through the bonding and finally lead to a failure of the complete junction. During the research project the behavior under cyclic loads was examined based upon coupon and detail test as and accompanied by high-fidelity FE-examinations. All results showed that the new design principle is in-sensitive to repeated loads and arrested growth can be shown in a basic level. As for time constraint reasons only, a few tests were performed on detail level with repeated loads and simplifications were introduced in the detail tests, a full demonstration of arrested growth for the *Aeropaste 1006* under shear and tension load is to be demonstrated in future.

First studies about weight and manufacturing cost of this type of bond line is extremely promising as related to a running length of the bond line itself the cost can be reduced by 30% and the weight up to even 50% compared to a classical bolted joint connection especially when countersink fasteners are used. The main driving parameters for the weight saving are two aspects: At first that for countersunk rivets the thickness of the panels needs to be increased locally in order to have a flush outer surface. Second is that due to the continuous load transfer (instead of the discrete one in case of rivets) the width of the frame flange can be reduced significantly as no edge distances have to be kept.

Additional advantages are that in the FAL no drilling operations with creation of chips are to be performed, that a possible repair, should it be necessary, can be performed by introducing a small bolt with protruding head, and no notch factors create weak points on frame's flanges which are normally acting as splice plate in this type of joints.

In summary it can be stated that the principle of the sub-division of the bond-line along its length is a very promising means to join panels in a damage tolerant manner. It offers the potential to be certifiable as with the separation into sub-bondings a possible crack cannot grow bigger than a certain size and is arrested in its growth reliably at the intersection line.

Future work has to be performed in order to have the full visibility of all influencing parameters in detail and to find the best pattern or shape respectively for a stress-optimized load transfer. Beyond the shapes given in this presentation other very promising shapes are under examination. In addition, the behavior under high-speed impact has to be examined in order to characterize this type of boding for crash-zones. Practical efforts have to be made in order to implement the design into a serial product in industrial size and environment.

8. Conclusions

1) Based upon a purely geometrical principle of splitting-up a bond-line along its running length, a simple and effective damage tolerant design principle was established: an intermeshing pattern which stops possible crack-growth in the bond line effectively.
2) As secondary but very beneficial effect the new pattern decreases the complete stress level in the bond line significantly (in both, shear and peel).
3) The basic principle was proven to work based upon thorough finite-element analyses and tests.
4) Tests were carried out on coupon and detail level in static and under repeated loads and proved the functionality of the developed principle.
5) With a simulated damage consisting of a complete missing triangle (=one failed sub-bond) the damage did not start to grow in the adjacent triangles and thus no-growth beyond one triangle is shown by test.
6) Even with several failed sub-bondings (i. e. removal of triangular sub-bondings) the specimen was able to transfer LL without failure. Up to a certain level even UL was reached.
7) A first conservative design and sizing rule for this new design principle is established.
8) The principle to generate damage tolerance can be transferred to any other positive substance jointing principle (p. e. thermoplast weding).

Author contact:

Martin Blacha: *martin.blacha@airbus.com*

Thomas Joachim: *thomas.joachim@airbus.com*

9. ACKNOWLEDGMENTS

The authors want to acknowledge the German Government for funding the research on damage tolerant structural bonding in the national LuFo-research project JoinDT. As well the authors like to acknowledge all contributors within Airbus Helicopters and the associated partners in industry and at research centers, especially to Deutsches Zentrum für Luft- und Raumfahrt (DLR, Braunschweig), Hochschule für angewandte Wissenschaften (HAW, Hamburg), Institute für Flugzeugbau (ifb, Stuttgart) and the Institut für Materialforschung und Anwendungstechnik (IMA, Dresden).

10. REFERENCES

1. O. Volkersen, O., „Die Nietkraftverteilung in zugbeanspruchten Nietverbindungen mit konstanten Laschenquerschnitten", Luftfahrtforschung 15.1/2 (1938), pp. 41–47.

2. Goland, M., and Reissner, E., "The stresses in cemented joints", Journal of Applied Mechanics 11.1 (1944), A17–A27.

3. Hertel, H.; Volkersen, O., US Patent 3,545,795, 1969.

4. Hart Smith, J., "Adhesive bonded scarf and stepped-lap joints", Tech. rep. Langley Research Center, NASA, 1973.

5. X. Zhao, X., Adams, R., and Da Silva L., “Single lap joints with rounded adherend corners: experimental results and strength prediction”, Journal of Adhesion Science and Technology 25.8 (2011), pp. 837–956.
6. Habenicht, G., „Kleben: Grundlagen, Technologien, Anwendungen“, VDI-Buch, Springer 2002.
7. Sachse, R., „Untersuchungen zur Auslegung von schadenstoleranten Klebeverbindungen durch mechanische Riss-Stopper-Elemente“. PhD thesis, University of Stuttgart, Stuttgart, 2019.
8. M. Blacha, S. Büsing, T. Joachim, “A basic principle for damage tolerant structural bonding in aerospace industry”, proceedings of the ECCM21 – 21st European Conference on Composite Materials, Nantes, 02-05 July 2024.
9. O. Völkerink, J. Kosmann, M. J. Schollerer, D. Holzhüter & C. Hühne (2019): Strength prediction of adhesively bonded single lap joints with the eXtended Finite Element Method, The Journal of Adhesion, DOI: 10.1080/00218464.2018.1553120
10. O. Völkerink, E. Petersen, J. Koord, C. Hühne, „A pragmatic approach for a 3D material model considering elasto-plastic behaviour, damage initiation by Puck or Cuntze and progressive failure of fibre-reinforced plastics“, article in “Computers and Structures”, Elsevier, 2020.
11. R. Sachse, A. K. Pickett, , W. Essig, , P. Middendorf, “Experimental and numerical investigation of the influence of rivetless nut plate joints on fatigue crack growth in adhesively bonded composite joints”, International Journal of Fatigue, Elsevier, 2017.

Supported by:

Federal Ministry
for Economic Affairs
and Climate Action

on the basis of a decision
by the German Bundestag